Dalton Transactions

ROYAL SOCIETY OF CHEMISTRY

COMMUNICATION

View Article Online
View Journal | View Issue

Cite this: *Dalton Trans.*, 2023, **52**, 3265

Received 8th February 2023,
Accepted 16th February 2023

DOI: 10.1039/d3dt00408b

rsc.li/dalton

Solid state luminescence of phosphine-EWO ligands with fluorinated chalcone skeletons and their PdX_2 complexes: metal-promoted phosphorescence enhancement†

Jaime Ponce-de-León, [a] Marconi N. Peñas-Defrutos, *[a] Andrea Vélez, [a] Gabriel Aullón [b] and Pablo Espinet *[a]

Complexes *trans*-[PdX_2L_2] (X = Cl and Br), where *L* is 1-(PR_2),2-(CH=CH–C(O)Ph)-C_6F_4 (R = Ph, Cy, and iPr), display phosphorescent emission in the solid state, whereas due to their substantially lower lifetimes, the free ligands exhibit fluorescent behaviour. Alternatively, structurally identical derivatives with halide replaced by CN^- or Pd replaced by Pt are non-emissive. DFT calculations explain this diverse behaviour, showing that the hybridization of orbitals of the MX_2 moiety with those of the chalcone fragment of ligands is significant only for the LUMO of the emissive compounds. In other words, in our complexes, only ML_MCT processes (L_M = Metal-perturbed Ligand-centered orbital) lead to observable luminescence.

Chalcone derivatives (Ar–CH=CH–CO–Ar') are mainly known for their biological activity and pharmacological applications,[1] but some of them also display interesting photophysical properties.[2] These compounds typically exhibit aggregation-induced emission due to lack of planarity that hinders π-stacking interactions and *push–pull* conjugation effects at the enone moiety,[3] which are the subject of very recent studies. Two reviews[3,4] and three relevant reports have been published in the last two years. Thus, the rare crystal jumping behaviour has been found for a highly luminescent chalcone derivative due to a reversible intermolecular [2 + 2] cycloaddition process in the solid state.[5] Moreover, chemosensors with chalcone-based chromophores have been applied for the selective detection of Cu^{2+} in aqueous media.[6] Besides, there is a report on the application of chalcone-derived liquid crystals for NH_3(g) sensing.[7]

Our pursuit of hemilabile ligands able to promote challenging Pd-catalysed C–C couplings (*e.g.* Ar^F–$Ar^{F'}$, Ar^F = fluorinated aryl) led us to develop the family of fluorinated PEWO ligands shown in Fig. 1A (PEWO = Phosphine bearing Electron-Withdrawing Olefins). The previously synthesized $\mathbf{L^1}$,[8] $\mathbf{L^2}$,[9] and $\mathbf{L^3}$, reported herein for the first time, differ in the PR_2 substituents (R = Ph, Cy, and iPr respectively), while the analogue of $\mathbf{L^1}$ labelled as $\mathbf{L^4}$, reported by Lei *et al.*, (Fig. 1B), lacks fluorine substitution.[10] All these PEWO ligands have a chalcone skeleton highlighted in red in Fig. 1. The hybrid chelating ligand $\mathbf{L^1}$ is extremely efficient in lowering the C–C reductive elimination barriers and allows for oxidative addition under catalytic conditions with either Ar–I or Ar–Br (Ar–Cl cannot be used).[11,12] Particularly, the *Z*-chelated complex [$PdCl_2L^1$] ($\mathbf{2L^1}$) is an active catalyst for the Negishi heterocoupling of perhaloaryls.[13]

The remarkably low activation barrier for *E*/*Z* olefin-isomerization (it occurs at room temperature) supports the extraordinary electronic delocalization of the double bond into both extremes (C_6F_4 and COPh) of our fluorinated chalcone phosphines (Scheme 1).[9,14] The latter confirms the special *pull–pull* conjugation in our R-PEWO-F_4 ligands, which is presumably related to the solid-state luminescence reported herein, displayed by the free ligands and some of their metal complexes, clearly enhanced by fluorination in the EWO.

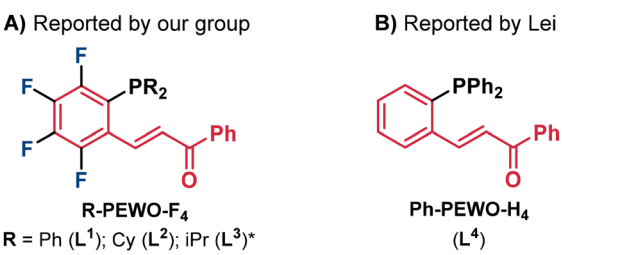

Fig. 1 Hybrid phosphine-EWO ligands used in this work with the chalcone group highlighted in red. A) Fluorinated derivatives (*$\mathbf{L^3}$ has not been previously reported). B) Non-fluorinated Ph analogue.

[a]*IU CINQUIMA/Química Inorgánica, Facultad de Ciencias, Universidad de Valladolid, 47071-Valladolid, Spain. E-mail: marconi_44@hotmail.com, espinet@qi.uva.es*

[b]*Secció de Química Inorgànica (Departament de Química Inorgànica i Orgànica), Institut de Química Teòrica i Computacional, Universitat de Barcelona, 08028 Barcelona, Spain*

†Electronic supplementary information (ESI) available: Synthesis and characterization of the complexes including NMR spectra, computational details and X-ray data. CCDC 2205013–2205017. For ESI and crystallographic data in CIF or other electronic format see DOI: https://doi.org/10.1039/d3dt00408b

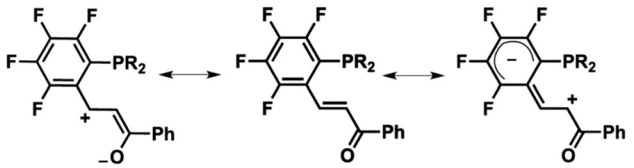

Scheme 1 Resonance forms contributing to the electron deficiency of the C=C double bond of the chalcone fragment.

Complexes *trans*-$[PdCl_2(L^n)_2]$ ($\mathbf{1L^{1-4}}$) show monodentate P-coordination and *E* configuration of the non-coordinated olefin, similar to the free ligands (Fig. 1). These compounds were selectively prepared by the reaction of *trans*-$[PdCl_2(NCMe)_2]$ with the appropriate PEWO in a Pd : L^n = 1 : 2 ratio (Scheme 2). Conversely, the reaction using a Pd : L^1 = 1 : 1 ratio eventually leads to the formation of an *E*-chelated intermediate (***E*-2L¹**), which subsequently isomerizes to the *Z*-chelated complex *cis*-$[PdCl_2(L^1)]$ (***Z*-2L¹**). The Z-configuration of ***Z*-2L¹** eventually triggers a C–F activation process, which opens the gate to new reactivity.[15]

Treatment of **1L¹** with KBr or AgCN yields *trans*-$[PdBr_2(L^1)_2]$ (**3L¹**) and *trans*-$[Pd(CN)_2(L^1)_2]$ (**4L¹**), respectively. The platinum compound *trans*-$[PtCl_2(L^1)_2]$ (**5L¹**) was synthesized analogously to **1L¹** (Scheme 2). In all compounds (free ligands and *trans*-$[MX_2(L^n)_2]$ complexes), the uncoordinated olefin group has the *E*-EWO configuration. The only exception is the chelate complex $[PdCl_2(Z\text{-}L^1)]$ (***Z*-2L¹**), which is coordinated by the P atom and the double bond, which display a *Z*-EWO conformation. The X-ray structures of **1L¹** (Fig. 2),[8] ***Z*-2L¹**,[8] **L²**,[9] and **1L⁴**,[16] are available in the literature, whereas those of ligand Ph-PEWO-F_4 (**L¹**) and complexes **1L²** and **1L³** (Fig. S1, ESI†) are first reported herein.

Neither the free ligands nor their complexes display emitting behaviour in solution,[17] whereas Table 1 presents the experimental data (excitation and emission maxima, average lifetimes, and quantum yield percentages) measured for the crystalline solids, where some remarkably intense emissions are observed. The emission spectra as well as the decay profiles are given in the ESI (Fig. S4–S13†).

The fluorinated ligands **L¹** and **L²** show yellow emission in the solid state upon UV irradiation, while the *E*-complexes **1L¹⁻³** and **3L¹** show eye-catching orange luminescence under similar conditions (*vide infra*, Fig. 3). However, the chelated *Z*-complex **2L¹**, showing a drastic structural divergence, does not exhibit emissive properties. The lack of fluorination is clearly detrimental to the luminescence (see quantum yield percentages of **L⁴** and **1L⁴** presented in Table 1), and more interestingly, both **4L¹** and **5L¹** complexes, which do not show any remarkable structural differences with **1L¹**, are not luminescent. Fig. 2 compares those three X-ray structures, including relevant distances within the chalcone ring (*i.e.* –C=C–) and involving the metal centres.

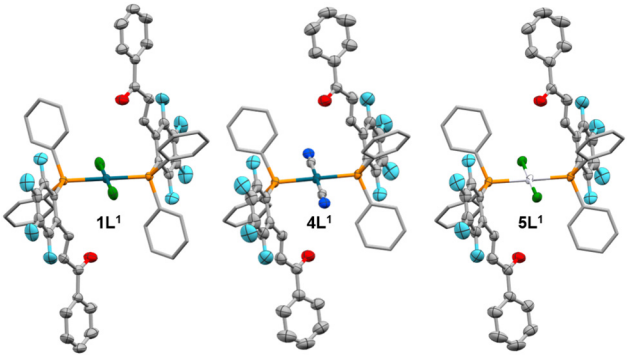

Fig. 2 X-ray structures of **1L¹**, **4L¹** and **5L¹**. H atoms omitted for clarity. Relevant distances in Å: **1L¹** : Pd–Cl = 2.2903(7), Pd–P = 2.3231(7), C=C (olefin) = 1.314(4). **4L¹** : Pd–C = 1.990(4), Pd–P = 2.3388(10), C=C (olefin) = 1.320(6). **5L¹** : Pt-Cl = 2.3029(11), Pt–P = 2.3241(11), C=C (olefin) = 1.303(7).

Table 1 Excitation and emission data of ligands and complexes in the solid state. Instability of L^3 under air (when non-coordinated) precludes its corresponding luminescence analyses

Entry/Comp.	λ_{exc} (nm)[18]	λ_{emis} (nm)[a]	Φ (%)	τ_{av} (ns)[b]
1/**L¹**	413	606	10.1	2.5
2/**L²**	460	530	4.1	3.5
3/**L⁴**	472	552	<3	3.0
4/**1L¹**	405	649	28.0	1.3×10^3
5/**1L²**	412	676	21.8	1.6×10^3
6/**1L³**	405	643	15.6	1.4×10^3
7/**1L⁴**	469	680	<3	6.4×10^2
8/***Z*-2L¹**	**Undetected emission**			
9/**3L¹**	415	666	15.7	5.1×10^3
10/**4L¹**	**Undetected emission**			
11/**5L¹**	**Undetected emission**			

[a] Very broad emission bands. [b] $\tau_{av} = (A_1\tau_1^2 + A_2\tau_2^2 + \cdots)/(A_1\tau_1 + A_2\tau_2 + \cdots)$.

In the free phosphine ligands, the chalcone moiety is clearly affected by the orbital influence of the R substituents at the P atom, as supported by the variations in their λ_{emis} values (Table 1, entries 1–3). In the complexes, additional dependence on the MX_2 metal fragment at which phosphine is coordinated is obvious (Table 1, entries 4–11).

Concerning the free ligands, the emissive transitions are necessarily intraligand. The effect of R substituents at P, with different electronic and steric features, is appreciable. The highest maximum wavelength (λ_{emis} = 606 nm) is found for the fluorinated **L¹** (R = Ph, entry 1). Note that the emission bands given in Table 1 are very broad and λ_{emis} is not enough to

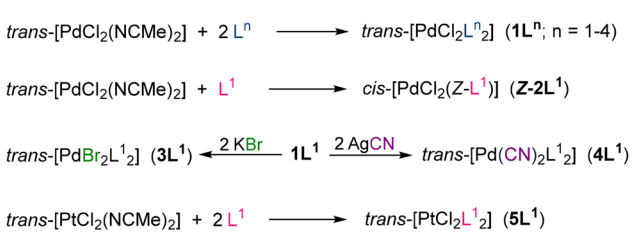

Scheme 2 Synthesis of *trans*-$[MX_2(L^n)_2]$ complexes $1L^n$ (n = 1–4), ***Z*-2L¹**, **3L¹**, **4L¹** and **5L¹**.

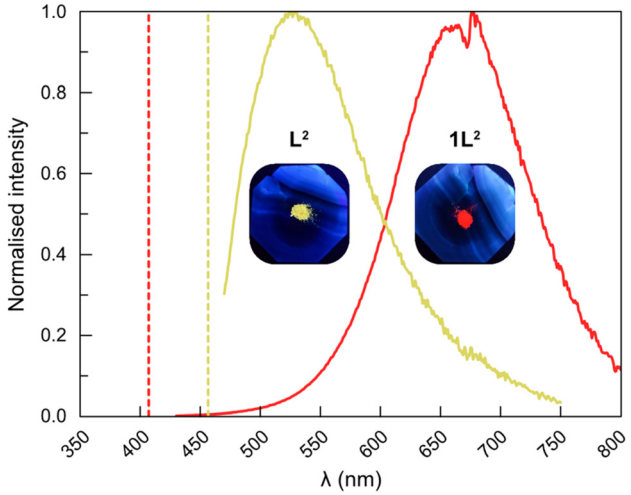

Fig. 3 Emission spectra, with normalised intensity, of the fluorinated ligand $\mathbf{L^2}$ (yellow line) and its $PdCl_2$ complex $\mathbf{1L^2}$ (red line); dashed lines represent the maximum of excitation (λ_{exc} in Table 1).[18] Photographs of a sample in a mortar, taken upon UV irradiation, are also shown.

guess the colour ($\mathbf{L^1}$ is yellowish upon irradiation too, see Fig. S3, ESI†). For the fluorinated $\mathbf{L^2}$ (R = Cy, λ_{emis} = 530 nm, Fig. 3), the wavelength is closer to the value obtained for the non-fluorinated Ph-PEWO-H_4 ligand $\mathbf{L^4}$ (entry 3) than for $\mathbf{L^1}$, as if the higher inductive effect of Cy acting as a σ-donor towards the P atom was compensating the electron-withdrawing effect of fluorination at the chalcone aryl group. Apparently, the two effects that should increase the σ-electron density at the chalcone ring (non-fluorination and inductive effect from R) diminish the quantum yield Φ values noticeably, to almost extinction in $\mathbf{L^4}$.

Remarkably, the colour change upon ligand coordination (yellow to orange) is linked to a substantially higher $\nu_{exc} - \nu_{emis}$ difference (*i.e.* 9.5 × 10^3 cm^{-1} *vs.* 2.9 × 10^3 cm^{-1} for $\mathbf{L^2}$ and $\mathbf{1L^2}$ respectively) and longer lifetimes (in the order of μs for the complexes and ns for the ligands). Fig. 3 shows the comparison between $\mathbf{1L^2}$ and $\mathbf{L^2}$. These observations suggest a luminescence switch upon coordination to $PdCl_2$, from fluorescence in the free ligands to phosphorescence in the complexes.[19]

Considering now the metal compounds, a remarkable increase in the quantum yield percentages (Φ > 15%, up to 28% for $\mathbf{1L^1}$), compared to the free ligands (Φ < 10%), is observed upon complexation to $PdCl_2$ in $\mathbf{1L^{1-3}}$ (Table 1, entries 4–6) or to $PdBr_2$ in the case of $\mathbf{3L^1}$ (Table 1, entry 9). In contrast, the non-fluorinated $\mathbf{1L^4}$ complex (Table 1, entry 7) is scarcely luminescent. This observation supports the important effect of the fluorine substituents of the chalcone ring on the emissive properties.[20]

In the case of the non-luminescent complexes $\mathbf{4L^1}$ and $\mathbf{5L^1}$, obviously their structural similarity with $\mathbf{1L^1}$ (Fig. 2) does not impede significant orbital differences when Pd or the halides are replaced by Pt or CN. The $PdCl_2$ ($\mathbf{1L^{1-3}}$) and the $PdBr_2$ ($\mathbf{3L^1}$) complexes have two medium-strength σ-donor and slightly π-donor halo ligands, and show similar λ_{emis} (nm) and Φ (%) values, as given in Table 1. Complex $\mathbf{4L^1}$ (Table 1, entry 10) has more σ-donor and very strongly π-acceptor cyano ligands. However, $\mathbf{5L^1}$ (Table 1, entry 11) has Pt replacing Pd, and the lanthanide contraction plus the relativistic effects in Pt produce large orbital energy differences between the Pd and Pt isoelectronic metal centres. Qualitatively, these two cases ($\mathbf{4L^1}$ and $\mathbf{5L^1}$) are roughly similar, because both compounds are expected to have a metal centre greedier of electron density and, consequently, less prone to be polarized by π back-donation towards the phosphine ligand.

In order to identify the orbitals involved in the absorption and emission, as well as to support our qualitative hypotheses, DFT and TD-DFT calculations were carried out (see ESI for details†). We focused the analysis on the ligand $\mathbf{L^1}$ and the complexes $\mathbf{1L^1}$, $\mathbf{4L^1}$, and $\mathbf{5L^1}$. As the emissions of $\mathbf{L^1}$ and $\mathbf{1L^1}$ are only observed in the solid state, their X-ray structures are used as initial guesses for geometry optimizations in the gas phase, which led to minimal modifications of the solid structures.

The computed HOMO–LUMO gap fits well the experimental λ_{exc} measured for $\mathbf{L^1}$ (λ_{calc} = 402 nm; λ_{exp} = 413 nm). The HOMO orbital is mainly located in the Ph_2P moiety and the LUMO is a chalcone orbital with high participation of fluorinated C atoms and those of the double bond (Fig. S17, ESI†). However, the computed wavelengths of the deexcitations from triplet states are far from the experimentally observed emission ($\mathbf{L^1}$, λ_{exp} = 606 nm), discarding them to assign a phosphorescent behaviour. There is, however, a $S_1 \rightarrow S_0$ transition from a singlet state, where slight structural bending of the chalcone group is suggestive of loss of sp^2 character of the double bond, which predicts an emission from π*(EWO) at λ_{calc} = 580 nm, much closer to the experimental value. Its fluorescent nature is strongly supported by the short lifetime of *ca.* 2 ns. In this transition, the participation of the R_2P fragment in the orbitals involved is significant (Table S12†). This is consistent with the experimentally observed effect of the R substituents at P.

The simulation of the absorption spectra allows us to assign the electronic transition from HOMO-2 to the LUMO orbital as responsible for the excitation maxima observed for $\mathbf{1L^1}$. The calculated transition (λ_{calc} = 395 nm) matches reasonably well the experimentally observed λ_{exc} maximum (405 nm, Table 1, entry 4). The contribution of the different molecular moieties is 58% Ph_2P + 22% $PdCl_2$ + 20% EWO for HOMO-2 (Fig. S18†) and 42% $PdCl_2$ + 38% EWO + 20% Ph_2P for LUMO (Fig. 4). Both orbitals are symmetrical, with equal contribution of the two ligands. Remarkably, similar transitions (HOMO-2 to LUMO) are computed to be markedly more energetic either in the Pt analogue $\mathbf{5L^1}$ (λ_{calc} = 349 nm) or in the $Pd(CN)_2$ complex $\mathbf{4L^1}$ (λ_{calc} = 333 nm), confirming the qualitative interpretation of similar behaviour of these two complexes (see Fig. S19 and S20 for MOs†).

Using TD-DFT calculations, the experimentally observed emission for $\mathbf{1L^1}$ (λ_{emis} = 649 nm, Table 1, entry 4) is assigned to the computed monodeexcitation from the first triplet state (T_1), with a much similar wavelength (λ_{calc} = 667 nm, Table S9, ESI†). This emission band mainly involves the LUMO →

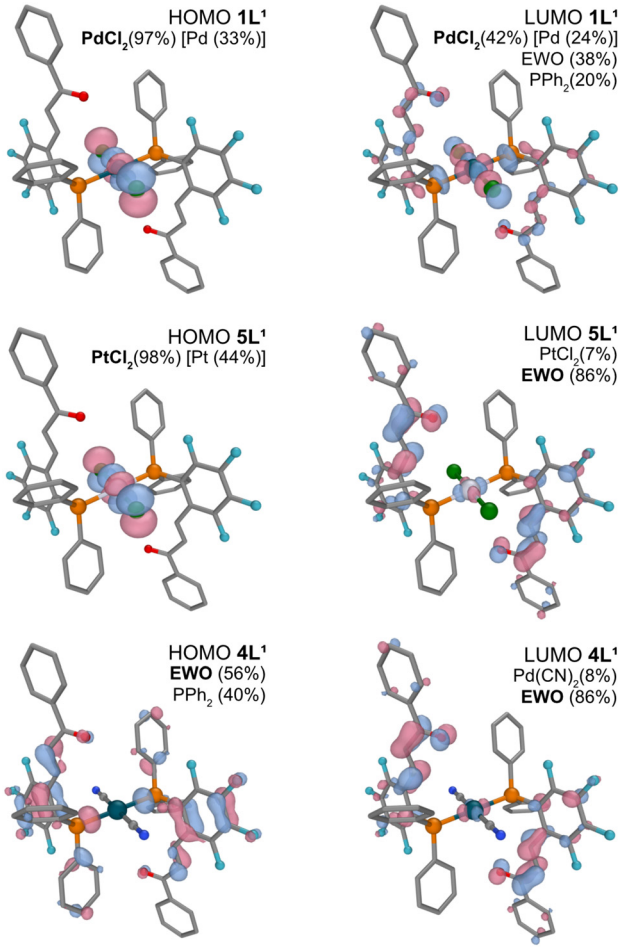

Fig. 4 FMOs of $\mathbf{1L^1}$ (top), $\mathbf{5L^1}$ (middle) and $\mathbf{4L^1}$ (bottom). Contributions (%) of the fragments are included, with the main participation in each case highlighted in bold. Relevant metal atom contributions (higher than 10%) are also shown.

HOMO phosphorescent transition. This is perfectly consistent with the high $\nu_{exc} - \nu_{emis}$ difference and the long lifetime values provided in Table 1 and commented previously. It is worth remarking that geometry relaxation was discarded due to the very limited deformability allowed in the solid state.[21] Moreover, the fluorescent emissions as well as other potentially phosphorescent ones were also computed and then discarded because of numerical results far from the experimental data (details in ESI†).

Fig. 4 gathers the frontier molecular orbitals (FMOs) of $\mathbf{1L^1}$, $\mathbf{4L^1}$ and $\mathbf{5L^1}$ for comparison. Evidently, deexcitation from the LUMO (42% $PdCl_2$, 38% EWO, 20% Ph_2P) to the $PdCl_2$ HOMO (Fig. 4, top), responsible for the orange-emitting behaviour of $\mathbf{1L^1}$, is drastically affected either in the $PtCl_2$ or in the $Pd(CN)_2$ analogues. The computed phosphorescent emissions (decay from triplet states) become experimentally unobservable for $\mathbf{4L^1}$ and $\mathbf{5L^1}$ (Tables S10 and S11 respectively†), as a direct consequence of the changes in the FMOs. For $\mathbf{5L^1}$ (Fig. 4, middle), the $PtCl_2$ HOMO resembles its $PdCl_2$ analogue but the contribution of the $PtCl_2$ fragment in the LUMO drops to 7% (*vs.* 42% for $\mathbf{1L^1}$) and the deexcitation from the first triplet is computed to be much more energetic (*i.e.* 555 nm). The effect of Cl by CN substitution in $\mathbf{4L^1}$ FMOs is also clear (Fig. 4, bottom), with reduced participation of the $Pd(CN)_2$ fragment in the LUMO of $\mathbf{4L^1}$ (casually almost identical to the $PtCl_2$ compound) and negligible in the HOMO.

After the identification of the key orbitals involved in the luminescent behaviour (with relevant participation of the $PdCl_2$ fragment), the data provided in Table 1 can be better rationalized: (i) both the $PdBr_2$ substitution in $\mathbf{3L^1}$ (Br is electronically quite similar to Cl) or the R_2P modification in $\mathbf{1L^2}$ and $\mathbf{1L^3}$ move in the range of variations of orbital polarization; (ii) totally different emission wavelengths must be expected from the Pd $(CN)_2$ ($\mathbf{4L^1}$) or $PtCl_2$ ($\mathbf{5L^1}$) congeners, with negligible contribution of the MX_2 moieties in their LUMOs. In fact, these happen not to be experimentally detectable. While many examples of either MLCT (MLCT = Metal to Ligand Charge Transfer) or ILCT (IL = Intra-Ligand Charge Transfer) emitting metal compounds can be found in the literature; in our system, only ML_MCT processes (L_M = Metal-perturbed Ligand-centered LUMO)[22] lead to observable phosphorescence.

In summary, we reported herein a family of yellow fluorescent 1-(PR_2),2-(CH═CH–C(O)Ph)-C_6F_4 chalcone-derived phosphines (L^n) and some intensely orange phosphorescent *trans*-$[PdX_2L^n{}_2]$ palladium(II) complexes (X = Cl and Br) with them displaying quantum yields (Φ) above 15%. The luminescence is only observed in the solid state and is enhanced by the fluorination in chalcone, both in the ligand and in the $PdCl_2$ complex. Using TD-DFT calculations, the emission of the free Ph-PEWO-F_4 ligand ($\mathbf{L^1}$) is assigned to the $S_1 \rightarrow S_0$ transition presumably associated with a loss of sp^2 character of the olefinic C atoms. Computational studies reproduce the excitation and emission data of the $PdCl_2$ compound $\mathbf{1L^1}$ satisfactorily and reveal the decisive involvement of the LUMO orbital, which features a clear metal/chalcone connection, in the luminescent behaviour. Conversely, the non-emitting Pd $(CN)_2$ and $PtCl_2$ analogues, structurally identical to $\mathbf{1L^1}$, display LUMO orbitals with scarce participation of the metal centres, supporting the synergistic contributions of both the MX_2 core and the chalcone skeleton in the emissive properties.

Conflicts of interest

There are no conflicts to declare.

Acknowledgements

We thank the Spanish MCINN (Projects PID2020-118547GB-I00 and PGC 2018-093863-B-C21) for the funding provided and both Eric Mates-Torres and Marta Mansilla (UBU) for help. J. P.-de-L. also acknowledges MCINN for a FPI studentship (BES-2017-080726). M. N. P-D. thanks the UVa for a Margarita Salas postdoctoral fellowship (ref. CONVREC-2021-221).

References

1 (*a*) C. Zhuang, W. Zhang, C. Sheng, W. Zhang, C. Xing and Z. Miao, *Chem. Rev.*, 2017, **117**, 7762–7810; (*b*) N. A. A. Elkanzi, H. Hrichi, R. A. Alolayan, W. Derafa, F. M. Zahou and R. B. Bakr, *ACS Omega*, 2022, **7**, 27769–27786; (*c*) S. L. Gaonkar and U. N. Vignesh, *Res. Chem. Intermed.*, 2017, **43**, 6043–6077.

2 K. G. Komarova, S. N. Sakipov, V. G. Plotnikov and M. V. Alfimov, *J. Lumin.*, 2015, **164**, 57–63.

3 S. Kagatikar and D. Sunil, *Chem. Pap.*, 2021, **75**, 6147–6156.

4 P. Mahesha, N. S. Shetty and S. D. Kulkarni, *J. Fluoresc.*, 2022, **32**, 835–862.

5 X. Cheng, F. Yang, J. Zhao, J. Ni, X. He, C. Zhou, J. Z. Sun and B. Z. Tang, *Mater. Chem. Front.*, 2020, **4**, 651–660.

6 L. J. Gomes, T. Moreira, L. Rodriguez and A. J. Moro, *Dyes Pigm.*, 2022, **197**, 109845.

7 A.-T. Mohammad and W. R. Abbas, *RSC Adv.*, 2021, **11**, 38444–38456.

8 E. Gioria, J. M. Martinez-Ilarduya, D. Garcia-Cuadrado, J. A. Miguel, M. Genov and P. Espinet, *Organometallics*, 2013, **32**, 4255–4261.

9 M. N. Peñas-Defrutos, A. Vélez, E. Gioria and P. Espinet, *Organometallics*, 2019, **38**, 4701–4707.

10 X. Luo, H. Zhang, H. Duan, Q. Liu, L. Zhu, T. Zhang and A. Lei, *Org. Lett.*, 2007, **9**, 4571–4574.

11 E. Gioria, J. del Pozo, J. M. Martínez-Ilarduya and P. Espinet, *Angew. Chem., Int. Ed.*, 2016, **55**, 13276–13280.

12 E. Gioria, J. del Pozo, A. Lledós and P. Espinet, *Organometallics*, 2021, **40**, 2272–2282.

13 J. Ponce-de-León and P. Espinet, *Chem. Commun.*, 2021, **57**, 10875–10878.

14 A. Roque, J. C. Lima, A. J. Parola and F. Pina, *Photochem. Photobiol. Sci.*, 2007, **6**, 381–385.

15 M. N. Peñas-Defrutos, A. Vélez and P. Espinet, *Organometallics*, 2020, **39**, 841–847.

16 H. Zhang, X. Luo, K. Wongkhan, H. Duan, Q. Li, L. Zhu, J. Wang, A. S. Batsanov, J. A. K. Howard, T. B. Marder and A. Lei, *Chem. – Eur. J.*, 2009, **15**, 3823–3829.

17 For an example of luminescent chalcones in the solid state but not in solution see: L. Zhang, J. Liu, J. Gao, R. Lu and F. Liu, *RSC Adv.*, 2017, **7**, 46354–46357.

18 Excitation spectra of metal complexes are scarcely informative (Fig. S14 and S15†). λ_{exc} is assigned as the wavelength that maximizes the emission intensity.

19 J. M. Forward, D. Bohmann, J. P. Fackler Jr. and R. J. Staples, *Inorg. Chem.*, 1995, **34**, 6330–6336.

20 For a different case see: J. Ponce-de-León, R. Infante and P. Espinet, *Chem. Commun.*, 2021, **57**, 5458–5461.

21 Reoptimization of both S_1 and T_1 states led to profound structural change, presumably not accessible in the crystal.

22 This notation has been recently used in:T. Theiss, S. Buss, I. Maisuls, R. López-Arteaga, D. Brünink, J. Kösters, A. Hepp, N. L. Doltsinis, E. A. Weiss and C. A. Strassert, *J. Am. Chem. Soc.*, 2023, **145**, 3937–3951.